PHYSICAL REVIEW B **87**, 161119(R) (2013)

Dimer Mott insulator in an oxide heterostructure

Ru Chen,[1] SungBin Lee,[2] and Leon Balents[3]
[1]*Department of Physics, University of California, Santa Barbara, Santa Barbara, California 93106, USA*
[2]*Department of Physics and Centre for Quantum Materials, University of Toronto, Toronto, Ontario, Canada M5S 1A7*
[3]*Kavli Institute of Theoretical Physics, University of California, Santa Barbara, Santa Barbara, California 93106, USA*
(Received 17 January 2013; published 26 April 2013)

We study the problem of designing an artificial Mott insulator in a correlated oxide heterostructure. We consider the extreme limit of quantum confinement based on ionic discontinuity doping, and argue that a unique *dimer Mott insulator* can be achieved for the case of a single SrO layer in a $GdTiO_3$ matrix. In the dimer Mott insulator, electrons are localized not to individual atoms but to bonding orbitals on molecular dimers formed across a bilayer of two TiO_2 planes and are analogous to the Mott insulating state of Hubbard ladders, studied in the 1990s. We verify the existence of the dimer Mott insulator through both *ab initio* and model Hamiltonian studies, and find for reasonable values of Hubbard U that it is stable and ferromagnetic with a clear bonding/antibonding splitting of order 0.65 eV and a significant smaller Mott gap whose size depends upon U. The combined effects of polar discontinuity, strong structural relaxation, and electron correlations all contribute to the realization of this unique ground state.

DOI: 10.1103/PhysRevB.87.161119 PACS number(s): 75.70.−i, 71.30.+h, 73.20.−r, 73.21.Cd

Recently, the growth techniques from semiconductor physics, such as molecular beam epitaxy (MBE), have been increasingly applied to transition-metal and rare-earth materials to create correlated heterostructures.[1] The resulting atomic layer control promises the ability to design orbital, spin, and charge states, create new emergent phenomena, and study fundamental physics of correlated quantum states in unprecedented new ways. A first step in this direction would be the creation of the simplest and most dramatic manifestation of electron-electron interactions: the formation of a Mott insulator, a system which would be a metal according to band theory, but in which instead electrons localize because their motion is jammed by their mutual short-range Coulomb repulsion.

Mott insulators occur only when the electron density is commensurate with the underlying lattice, and typically an (odd) integer number of electrons per atom is required. A charge density of one electron per atom is enormous, reaching of order $n_{2d} \approx 7 \times 10^{14}$ cm^{-2} for a typical perovskite structure even if these electrons are confined to a single atomic layer. This provides a challenge for heterostructures, as this n_{2d} is already an order of magnitude larger than can be achieved in the highest density semiconductors, and even if it is created, the electron density per atom will be greatly reduced by the electron's tendency to spread out in the third dimension. In this paper, we show that these difficulties can be overcome by judicious design of a Dimer Mott insulator (DMI), a state envisioned decades ago in the context of one-dimensional Hubbard ladders,[2] and created here in two dimensions at a single monolayer of SrO embedded in a $GdTiO_3$ matrix. In the DMI, the requisite high charge density is achieved by combining ionic discontinuity doping, quantum confinement, and the formation of electronic dimers. The dimers are bonding orbitals on electron pairs, to which electrons are Mott localized instead of to individual atoms. Dimer formation halves the charge density needed to reach the Mott state, relative to the usual single-atom localization, and is crucial to the success of our scheme. We combine *ab initio* and model calculations to establish the existence and nature of the DMI state theoretically.

The starting point for our work is the polar/ionic discontinuity, which induces a large net charge, typically half an electron per planar unit cell, at a polar to nonpolar interface. The polar discontinuity has been identified as a possible mechanism of doping in many oxide interface studies,[1,3] but has only recently been quantitatively verified systematically.[4] In MBE grown heterostructures of $GdTiO_3$ and $SrTiO_3$, a carrier density of $n_{2d} = 3.5 \times 10^{14}$ cm^{-2} ($=\frac{1}{2}$ e^- per planar unit cell) for each $GdTiO_3/SrTiO_3$ interface has been systematically observed by Hall coefficient measurements.[4] These electrons fall into the empty d states of the $SrTiO_3$, and consequently high-3d carrier density can be achieved by confinement in narrow quantum wells of $SrTiO_3$ embedded in thicker $GdTiO_3$, with $n_{3d} = n_{2d}/w$, where w is the well width. Recent transport experiments[5] showed that such wells with a width of a few $SrTiO_3$ unit cells are indeed strongly correlated metals with ultrahigh carrier density $n_{2d} = 7 \times 10^{14}$ cm^{-2} arising from two interfaces, corresponding to $\frac{1}{2} + \frac{1}{2} = 1$ e^- per planar unit cell.

To maximize the 3d electron density and approach the Mott limit, we take this approach to its logical end and consider the case of a single SrO layer embedded in $GdTiO_3$. However, even in this case of ultimate confinement, we do not achieve a 3d density of 1 e^- per atom. This is because the doped electrons go symmetrically into the two interfaces TiO_2 layers on either side of the SrO plane. While this situation appears unfavorable for the formation of a Mott insulator, all is not lost. On fundamental grounds, the condition for the formation of a Mott state depends only on the charge per unit cell defined by the translational symmetry of the system. Here, the two interface planes form a bilayer, with translational symmetry only within the plane, and there is indeed a unit charge per planar unit cell. This indicates that a Mott state is possible in principle. To realize it, we must somehow induce the two Ti atoms in a unit cell to act as a single "superatom."

It is instructive to view the bilayer on its side, with the Ti atoms projected into an x-z plane (here we use standard cubic coordinates for the perovskite structure, and z is the growth direction). The Ti-O-Ti network then forms a ladder with Ti-O-Ti bonds between the two interfaces making the rungs of the ladder, and intraplane bonds projecting to the ladders legs. In a Hubbard model description, symmetry dictates that the hopping amplitude for electrons along the legs t and along the rungs $t_\perp$ are unequal. Correlated electron ladders were studied intensively in the 1990s,[2] and in particular it was shown when $t_\perp/t$ is sufficiently large (approximately $t_\perp/t > 1$ for the one-dimensional Hubbard ladder), electrons form an unconventional Mott state of bonding orbitals on the rungs of the ladder: the one-dimensional analog of the DMI. Qualitatively, we anticipate the same physics applies to the Hubbard bilayers, provided $t_\perp/t$ is sufficiently large.

Hopping parameters in transition-metal oxides are largely controlled by the metal-oxygen-metal bond angle, due to the directionality of d and p orbitals, and are generally largest when the bond angle is closest to 180°. Intuitively, we expect that the interlayer Ti-O-Ti bonds are the most $SrTiO_3$-like, while those within the TiO_2 planes conform more closely to those of the $GdTiO_3$. Since $SrTiO_3$ is nearly perfectly cubic, while $GdTiO_3$ is one of the most highly distorted titanates, this appears quite favorable. We checked this intuition with *ab initio* density functional theory (DFT) calculations for periodic superlattices of the single SrO layer $(SrTiO_3)_1(GdTiO_3)_n$ with $n = 3,5$. Calculations were performed in the WIEN2K (Ref. 6) implementation and the generalized gradient approximation[7] (GGA). An RKmax parameter 7.0 was chosen with muffin-tin radii (RMTs) of 1.91 a.u., 1.69 a.u., 2.29 a.u. and 2.27 a.u. for Ti, O, Sr, and Gd, respectively. The DFT calculation is carried out in a $\sqrt{2}a \times \sqrt{2}a \times c$ unit cell to allow for the possibility of octahedral tilts, where a is set to be the value of the experimental $SrTiO_3$ lattice constant, 3.905 Å (see the Supplemental Material[8] for additional details). The structural optimization is done both on the atomic coordinates and c/a ratio, within the GGA $+U$ approximation. We focus on $U_{\text{eff}} = U - J = 4$ eV on the Ti d orbitals, an acceptable value for the titanates.[9] In addition, we further add $U_{\text{eff}} = U - J = 8.5$ eV on the Gd f orbitals since the energy of the occupied Gd f bands lies much lower than the Fermi energy in practice. This value will not affect the relevant electronic properties.

We now discuss the key features of the relaxed structure, which becomes independent of n for $n \geqslant 3$, and is shown in Fig. 1. First, relaxation is significant at the two interface layers, but decays quickly into the $GdTiO_3$ region. Second, the Ti-O-Ti bond angles are highly direction dependent near the interface, as shown in Fig. 2. The "vertical" Ti-O-Ti bond connecting the two interfaces is slightly distorted, with a 160° angle. The next vertical Ti-O-Ti bond away from the interface is already highly distorted, with only a 3° angular difference from that of bulk $GdTiO_3$, and more distant bonds are nearly indistinguishable from bulk. On the other hand, the in-plane bonds are distorted but different from the bulk even in the interfacial layers, with bond angles of about 153°. Third, the Ti-O bond length varies by only 6% between the longest and shortest bonds in the entire superlattice, and is less significant compared to the dramatic bond-angle variations.

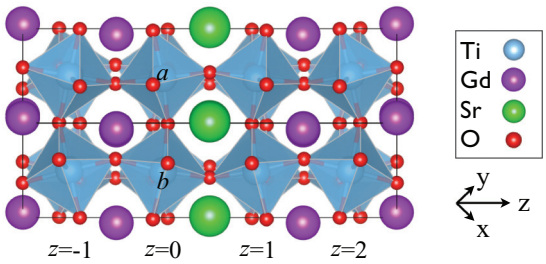

FIG. 1. (Color online) One unit cell of the relaxed structure of the superlattice $(SrTiO_3)_1(GdTiO_3)_3$. TiO_6 octahedra are drawn in blue, to emphasize tilts. The superlattice repeats periodically along the z direction. The bilayer consists of TiO_2 planes at $z = 0$ and 1. Here, a and b denote the two different Ti sublattices.

Is the bond-angle difference, together with other minor structural relaxation effects, sufficient to promote a DMI? We first check the electronic structure within the GGA$+U$ approximation using the relaxed structure. Searching for possible magnetic structures, we obtained the lowest energy for a state with ferromagnetic alignment of Ti spins within each TiO_2 plane, with interfacial Ti spins antiparallel to those in the $GdTiO_3$ region (energy difference compared to parallel to those in the $GdTiO_3$ region is small). With this configuration, and $U_{\text{eff}} = 4$ eV, the interfacial and bulk density of states (DOS) is shown in Fig. 3. We observe a bulk gap of 1.25 eV, comparable to theoretical values in the literature, but remarkably a much reduced but still nonzero gap at the interface of approximately 0.2 eV. This is a signature of the DMI state. Within GGA$+U$, the DMI persists for $U_{\text{eff}} \gtrsim 3.5$ eV, with both bulk and interfacial gaps reduced for smaller U. To see the DMI more directly, we decomposed the DOS by Ti site and the 3 t_{2g} orbitals (defined by pseudocubic axes). Within the interface plane, the major DOS just below the Fermi level has no xy character, consisting instead of spin-down predominantly xz/yz orbitals on alternating a/b sublattices. Consequently, we identify this state as the occupied bonding orbital of the DMI, with the xz/yz orbital degeneracy

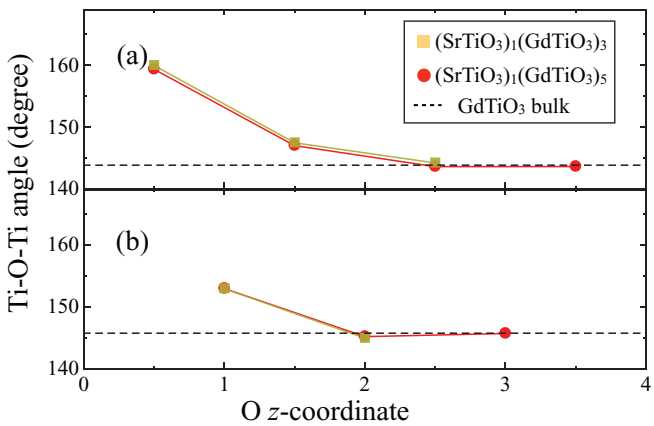

FIG. 2. (Color online) Ti-O-Ti bond angles along (a) vertical direction and (b) in-plane direction with respect to the O (in the Ti-O-Ti bond) z positions. O along vertical direction resides in the RO (R = Sr, Gd) plane, which is why the coordinate appears to be half-integer.

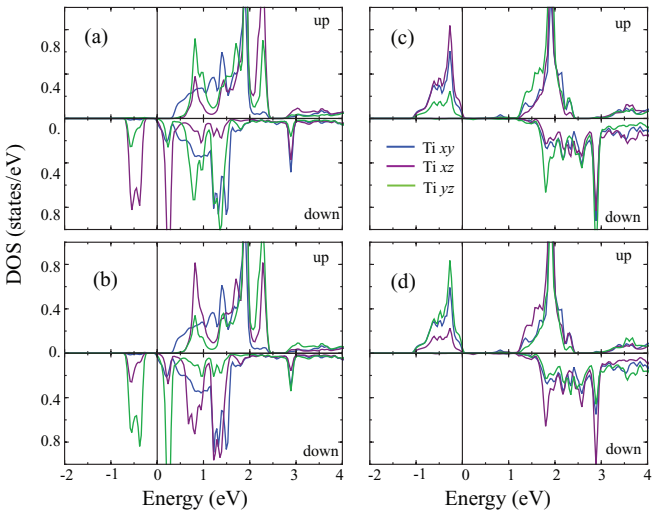

FIG. 3. (Color online) Layer-resolved electronic density of states of Ti $3d$ states of (a) sublattice a and of (b) sublattice b at $z = 1$ (at the interface); Ti of (c) sublattice a and of (d) sublattice b at $z = 2$ (center of $GdTiO_3$ region). The Fermi energy is set to zero.

split by octahedral rotations. The antibonding state, centered at around 0.2 eV, is again mainly composed of yz or xz orbitals. The separation (of subband centers) from the bonding state gives the bonding/antibonding splitting of 0.65 eV. The gap is much smaller than this splitting, however, due the width of the bonding and antibonding bands. Away from the interface region, the electronic structure resembles that of bulk $GdTiO_3$. For the Ti in the center of the $GdTiO_3$ region, we observe dominant xy/yz and xy/xz states alternating between two orthorhombic sublattices. Quantitative analysis shows the occupation at xy, yz, and xz states are 37%, 16%, and 47% for Ti at sublattice a, similar to in bulk $GdTiO_3$.

To study the DMI state more explicitly, we constructed a model extended Hubbard Hamiltonian by extracting hopping parameters from the *ab initio* calculations. Using the optimized structure obtained within GGA+U, a pure GGA calculation was carried out. The eigenvalues of the f states of Gd were shifted manually away from the Fermi energy. We constructed 30 maximally localized Wannier functions[10,11] (MLWF) around the Fermi energy, with the 3 t_{2g} orbitals forming the basis. The hopping parameters were then calculated by evaluating the matrix element of the MLWF. Including these hopping parameters, the tight-binding model of the bilayer takes the form

$$H_{\rm tb} = \sum_{\langle ij\rangle} \sum_{mn,\alpha} t_{ij}^{mn} c_{ima}^{\dagger} c_{jn\alpha}, \qquad (1)$$

where i and j are nearest-neighbor sites, m and n are orbital indices, and α is the spin index. The hopping parameters for the two interfacial Ti layers are tabulated in Table I, which contains the full orbital dependence of the hopping terms. The maximum intraplane and interplane hopping matrix elements are $t \sim 0.35$ eV and $t_\perp \sim 0.63$ eV, respectively, which gives strong support for the DMI picture. The separation energy between bonding and antibonding states is consistent with this magnitude interplane hopping.

TABLE I. Hopping parameters for two TiO_2 interface layers from fits to the $(SrTiO_3)_1(GdTiO_3)_3$ superlattice in units of eV. The index, for example $1ayz$, stands for sublattice a Ti at $z = 1$ with basis yz state. All the major hoppings (larger than 10% of the largest hopping magnitude) are kept here.

	Direction			Direction
$(im; jn)$	[1, 1, 0]	[−1, 1, 0]	$(im; jn)$	[0, 0, 1]
$(1ayz; 1byz)$	0	−0.35	$(0ayz; 1ayz)$	−0.6
$(1ayz; 1bxz)$	0.14	0.14	$(0ayz; 1axz)$	0
$(1axz; 1byz)$	−0.12	−0.12	$(0axz; 1ayz)$	0
$(1axz; 1bxz)$	−0.35	0	$(0axz; 1axz)$	−0.63
$(1axy; 1bxy)$	−0.34	−0.34	$(0axy; 1axy)$	0

We supplement these hopping parameters with interactions,[9,12] to form the effective Hamiltonian,[9,12]

$$H = H_{\rm tb} + H_{\rm int}$$

$$H_{\rm int} = \sum_i \Bigg[U \sum_m n_{im\uparrow} n_{im\downarrow} + U' \sum_{m\neq n} n_{im\uparrow} n_{in\downarrow} + \frac{1}{2}(U' - J) \sum_{m\neq n,\alpha} n_{ima} n_{in\alpha} + J \sum_{m\neq n} c_{im\uparrow}^{\dagger} c_{in\uparrow} c_{in\downarrow}^{\dagger} c_{im\downarrow} + J' \sum_{m\neq n} c_{im\uparrow}^{\dagger} c_{in\uparrow} c_{im\downarrow}^{\dagger} c_{in\downarrow} \Bigg], \qquad (2)$$

where U and U' represent onsite intraorbital and interorbital Coulomb repulsion between up and down spins, respectively, and J is the Hund coupling. We will not restrict the condition to Slater-Kanamori interaction parameter $U' = U - 2J$ and $J = J'$, but rather simply assume $J = J'$ and explore the phase diagram by varying all the other parameters.

Figure 4 shows the phase diagram as a function of U and U' obtained by the Hartree-Fock approximation, with fixed Hund's coupling $J = 0.6$ eV. When the Coulomb repulsion is small, the ground state is just paramagnetic metal. In the unphysical region where interorbital repulsion is dominant $U' > U$, electrons reside in a single orbital per Ti and in fact charge

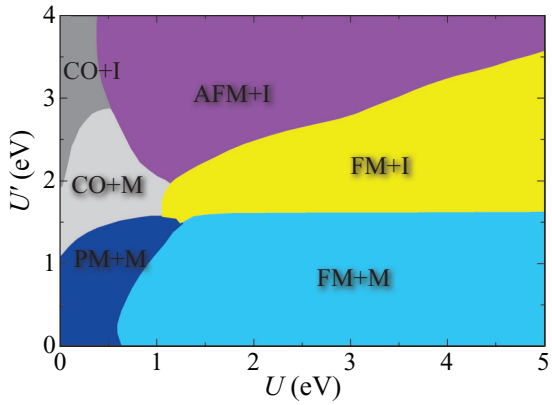

FIG. 4. (Color online) Hartree-Fock phase diagram for Hund's couping $J = 0.6$ eV. Here, we abbreviate the phases as follows: PM + M = paramagnetic metal; CO + M = weakly charge ordered metal; CO + I = charge ordered insulator; FM + M = ferromagnetic metal; FM + I = ferromagnetic insulator; AFM + I = antiferromagnetic insulator.

order. Of most interest is the lower right part of the phase diagram, where $U > U'$. In this region, ferromagnetism arises for sufficiently large U. In the weak interorbital repulsion limit, the electrons are distributed in all three t_{2g} orbitals. Under this condition, the system is always metallic or semimetallic since those electrons in xy orbitals are nonbonding between layers and hence metallic. For sufficiently large U', however, the interorbital repulsion eventually disfavors and empties the xy states, in favor of the xz/yz orbitals which have lower energy through interlayer hopping. In this way, the bonding state becomes fully occupied and a (ferromagnetic) DMI is achieved. Further increase of U' enhances the gap and eventually prefers an antiferromagnetic DMI since Hund's coupling becomes ineffective if there is strictly one electron per site, and superexchange becomes dominant. For completeness, we also have tested $J = 0,1$ eV, which shows the Hund's coupling enhances the ferromagnetic insulating state. For our best guess at physically appropriate values, e.g., $U = 4.5$ eV and the Slater-Kanamori $U' = U - 2J$, the ferromagnetic DMI obtains. The Hartree-Fock results for these values for the band gap and orbital ordering are very similar to those of the previously discussed GGA+U calculations.

In summary, we have argued for the existence of a Dimer Mott insulator (DMI) for a single SrO layer embedded in a thick $GdTiO_3$ matrix, using both *ab initio* and model calculations. The DMI state is unique to the bilayer TiO_2 structure created by a single SrO layer; we have indeed verified that a metallic state is obtained in GGA+U for the case of two SrO layers embedded in $GdTiO_3$ (see Supplemental Material[8]). Insulating behavior in such structures experimentally should therefore be attributed to the combined effects of disorder (e.g., $SrTiO_3$ thickness fluctuations) and interactions. The DMI for a single SrO layer could be experimentally probed by many experiments, including transport, optical measurements of the gap and bonding-antibonding splitting, and angle-resolved photoemission. Observing the magnetic structure is more difficult, but might be possible with ferromagnetic resonance or optical dichroism. This work suggests many directions for future theoretical and experimental research. We anticipate that the Mott state can be controlled and modified by varying composition, strain, and the growth direction. It may be possible to create antiferromagnetic DMIs by varying the rare-earth ion; however, theory is needed to gauge whether this also may destabilize the dimer formation itself. Choice of substrate also effects the strain and growth direction of the titanate films. Whether the DMI persists when the $GdTiO_3$ grows along the (110) direction is an important question for future study. More speculatively, we might contemplate the possibility of superconductivity induced by doping the DMI, by analogy to the superconductivity predicted theoretically and observed experimentally in ladder systems.

We thank J. Allen, S. Stemmer, D. Ouellette, P. Moetakef, and C.-H. Yee for helpful discussions. We acknowledge support from the Center for Scientific Computing from the CNSI, MRL: an NSF MRSEC (DMR-1121053) and NSF CNS-0960316. This research is supported by DARPA Grant No. W911-NF-12-1-0574 (L.B. and R.C.) and the MRSEC Program of the National Science Foundation, Award No. DMR 1121053, NSERC, CIFAR (S.B.L.).

[1] J. Mannhart and D. Schlom, Science **327**, 1607 (2010).
[2] E. Dagotto and T. M. Rice, Science **271**, 618 (1996).
[3] N. Nakagawa, H. Hwang, and D. Muller, Nat. Mater. **5**, 204 (2006).
[4] P. Moetakef, T. A. Cain, D. G. Ouellette, J. Y. Zhang, D. O. Klenov, A. Janotti, C. G. Van de Walle, S. Rajan, S. J. Allen, and S. Stemmer, Appl. Phys. Lett. **99**, 232116 (2011).
[5] P. Moetakef, C. A. Jackson, J. Hwang, L. Balents, S. J. Allen, and S. Stemmer, Phys. Rev. B **86**, 201102 (2012).
[6] P. Blaha, K. Schwarz, G. K. H. Madsen, D. Kvasnicka, and J. Luitz, *WIEN2k, An Augmented Plane Wave Plus Local Orbitals Program for Calculating Crystal Properties* (Vienna University of Technology, Austria, 2001).
[7] J. P. Perdew, K. Burke, and M. Ernzerhof, Phys. Rev. Lett. **77**, 3865 (1996).
[8] See Supplemental Material at http://link.aps.org/supplemental/10.1103/PhysRevB.87.161119 for (a) more DFT calculation details of the superlattices; (b) the *ab initio* results obtained for two SrO layers embedded in a $GdTiO_3$ matrix.
[9] T. Mizokawa and A. Fujimori, Phys. Rev. B **54**, 5368 (1996).
[10] A. Mostofi, J. Yates, Y. Lee, I. Souza, D. Vanderbilt, and N. Marzari, Comput. Phys. Commun. **178**, 685 (2008).
[11] J. Kuneš, R. Arita, P. Wissgott, A. Toschi, H. Ikeda, and K. Held, Comput. Phys. Commun. **181**, 1888 (2010).
[12] M. Imada, A. Fujimori, and Y. Tokura, Rev. Mod. Phys. **70**, 1039 (1998).